BULLETIN OF THE POLISH ACADEMY OF SCIENCES
TECHNICAL SCIENCES, Vol. 69(1), 2021, Article number: e136040
DOI: 10.24425/bpasts.2021.136040

Electromagnetic AC and impulse levitations of conductive, dielectric, and magnetic ball

Dariusz SPAŁEK*

Silesian University of Technology, Electrical Engineering Faculty, ul. Akademicka 10, 44-100 Gliwice, Poland

Abstract. The paper presents an analytical solution of levitation problem for conductive, dielectric and magnetically anisotropic ball. The levitation exerts either an AC or impulse magnetic field. Both the Lorentz and material electromagnetic forces (of magnetic matter) could lift the ball in a gravitational field. The electromagnetic field distribution is derived by means of variables separation method. The total force is evaluated by Maxwell stress tensor (generalized), co-energy and Lorentz methods. Additionally, power losses are calculated by means of Joule density and the Poynting vector surface integrals. High frequency asymptotic formulas for the Lorentz force and power losses are presented. All analytical solutions derived could be useful for rapid analysis and design of levitations systems. Finally, some remarks about considered levitations are formulated.

Key words: levitation forces; ball; AC and impulse electromagnetic fields; power losses.

List of main symbols

a_n, b_n, c_n, d_n	– constants for magnetic potentials
$\vec{A}$	– magnetic potential vector
B_0	– forced magnetic flux density (constant item)
B_r, B_θ, B_φ	– magnetic flux density components
C_1	– forced magnetic field gradient [T·m^{-1}]
f	– frequency
g	– acceleration of gravity 9.80665 m·s^{-2}
$\vec{i}_u$	– versor for u-th coordinate
m	– ball mass
$\vec{N}$	– material force density
R	– radius of the ball
s	– $= \pm 1/T + \mathrm{i}\omega$
$S_n(x)$	– polynomials for magnetostatic field solutions
$u, w \in \{r, \theta, \varphi\}$	– indices of spherical coordinate system
W_C	– co-energy
γ	– conductivity
ε_0	– dielectric permittivity of the vacuum
ε_{uw}	– dielectric permittivity of $u-w$ axes
μ_0	– magnetic permeability of the vacuum
μ_{uw}	– magnetic permeability of $u-w$ axes
ν_0	– reluctivity of the vacuum
ν_{uw}	– reluctivity of $u-w$ axes
σ_{uw}	– Maxwell stress tensor of $u-w$ axes
$\omega = 2\pi f$	– angular speed

1. Introduction

Analytical solutions of electromagnetic problems usually reveal a wide insight into the influence of all parameters on the field distribution and integral quantities, e.g. total force and power losses. In this paper some analytical solutions for levitations problems are derived for a wide range of frequency, conductivity, electric permeability and magnetic permittivities of the ball. The proposed solutions could be treated as accurate (default) solutions for the ball levitation problem. There are important reasons for applying the analytical solutions. Firstly, the explicit form of the solutions leads to simple integrals and asymptotic formulas (e.g. for rapid design). Secondly, the analytical solutions are benchmark tasks for numerical algorithms [1–5]. Thirdly, the analytical solutions constitute suitable start points for numerical methods that solve nonlinear problems. Moreover, the analytical solutions could reduce numerical costs while designing hybrid algorithms for electromagnetic problems.

The novelty of the analytical solutions presented involves considering:

- Material force appearing at the surface of a ball (not only the Lorentz force);
- Conductive, dielectric, and magnetic (anisotropic) parameters of a levitating ball;
- Both AC and impulse excitations;
- Asymptotic formulas for the Lorentz force and power losses at high frequency.

2. Electromagnetic and magnetic levitations

Electromagnetic levitation (of induced currents) and/or magnetic levitation (of magnetic matter) could lift an object in a

*e-mail: dariusz.spalek@polsl.pl

Manuscript submitted 2020-07-09, revised 2020-08-31, initially accepted for publication 2020-09-08, published in February 2021

gravitational field [1, 2, 5, 6]. Nowadays, both electromagnetic and magnetic levitations are of interest and wide attention.

Particularly, the levitation could be caused by:

- Lorentz force acting upon currents induced in a conductive probe (electromagnetic levitation, power losses [7, 8]);
- Material forces acting on the outer surface and/or inside an object, i.e. in regions where magnetic reluctivity changes [8–12]

as well as (not considered in this paper):

- Permanent magnets or electromagnets;
- The Poynting force outside of technical interests because of an extremely small value.

Exemplary levitation is used in high-speed trains, frictionless bearings, vibration isolation for sensitive actuators, medicine treatment, furnaces that enable for container-less melting of metal probe [5, 7].

In order to obtain a required value of levitation force (that exceeds the object weight) the imposed magnetic field has to be designed in a certain way. Particularly, it is necessary to exert magnetic field having both axial and radial components, set the frequency and consider the probe material and geometrical parameters.

3. Electromagnetic field analysis

Electromagnetic and magnetic levitations appear while electromagnetic forces could lift an object in a gravitation field, respectively. Particularly, the Lorentz forces act on currents induced in a conductive object. The material forces act on the surface of the magnetic object (made of either isotropic or anisotropic magnetic matter). Both the Lorentz and material forces lift the conductive and magnetic object if their sum is greater than the gravitational force mg (weight). Furthermore, it is assumed that forces exerted by magnetic hysteresis, magnets, and magnetic asymmetrical anisotropy do not appear [1, 2, 11, 13–16]. The Lorentz force is immanently bound up with the Joule power losses. The Joule power losses are often sufficiently high to melt the levitating object (e.g. a disc, a ball).

Let us consider a ball in a forced axially symmetric (Fig. 1) and alternating magnetic field imposed far from a ball given arbitrary by polynomial of N items [5, 7, 17–19]

$$B_z(t,z) = a(t)\left\{B_0 - \sum_{i=1}^{N-1} C_i z^i\right\}, \tag{1}$$

where B_0 and C_i are constants.

The Ampère-Maxwell law

$$\mathrm{curl}\vec{H} = \vec{J} + \frac{\partial \vec{D}}{\partial t} \tag{2}$$

for spherical coordinate system tangential component φ of (2) is as follows

$$\frac{\partial}{r\partial r}(rH_\theta) - \frac{\partial}{r\partial\theta}(H_r) = J_\varphi + \frac{\partial D_\varphi}{\partial t}. \tag{3}$$

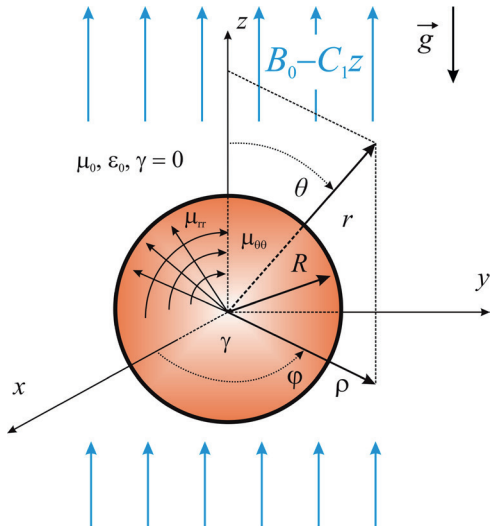

Fig. 1. Conductive and magnetic ball in axial magnetic field

Let us assume the ball is magnetically anisotropic in the diagonal form (for spherical coordinates system) as follows

$$\begin{bmatrix} H_r \\ H_\theta \\ H_\varphi \end{bmatrix} = \begin{bmatrix} \nu_{rr} & 0 & 0 \\ 0 & \nu_{\theta\theta} & 0 \\ 0 & 0 & \nu_{\varphi\varphi} \end{bmatrix} \begin{bmatrix} B_r \\ B_\theta \\ B_\varphi \end{bmatrix} = \begin{bmatrix} \nu_{rr}B_r \\ \nu_{\theta\theta}B_\theta \\ \nu_{\varphi\varphi}B_\varphi \end{bmatrix}, \tag{4}$$

thus

$$\frac{\partial}{r\partial r}(r\nu_{\theta\theta}B_\theta) - \frac{\partial}{r\partial\theta}(\nu_{rr}B_r) = J_\varphi + \frac{\partial D_\varphi}{\partial t}. \tag{5}$$

Magnetic flux density for symmetrically axial magnetic field can be described only by magnetic vector potential component A_φ

$$\vec{A} = A_\varphi \vec{i}_\varphi, \tag{6}$$

then

$$\vec{B} = \mathrm{curl}\vec{A} = \frac{\vec{i}_r}{r\sin\theta}\frac{\partial(A_\varphi \sin\theta)}{\partial\theta} - \frac{\vec{i}_\theta}{r}\frac{\partial(rA_\varphi)}{\partial r}. \tag{7}$$

Now, Eq. (5) can be rewritten in the following form

$$\frac{1}{r^2}\frac{\partial}{\partial r}\left(r^2\frac{\partial A_\varphi}{\partial r}\right) + \frac{\nu_{rr}}{r^2\nu_{\theta\theta}}\frac{\partial}{\partial\theta}\times \\ \times\left(\frac{1}{\sin\theta}\frac{\partial(A_\varphi\sin\theta)}{\partial\theta}\right) = \Gamma^2 A_\varphi. \tag{8}$$

where

$$\Gamma^2 = s\gamma\mu_{\theta\theta} + s^2\varepsilon\mu_{\theta\theta}, \tag{9}$$

and $\mu_{\theta\theta} = \nu_{\theta\theta}^{-1}$.

For sine field $\mathrm{a}(t) = \sin(\omega t)$ is set $s = \mathrm{i}\omega$. Then Eqs. (5) and (8) are applied for complex magnetic field vectors (RMS value equal to $1/\sqrt{2}$).

Ideal rectangular impulse field is satisfied with $T_1 \to 0$ and $T_2 \to 0$, as shown in Fig. 2a. The force of the impulse field can be evaluated considering that indeed $T_1 \neq 0$, $T_2 \neq 0$ where both

slopes are exponential (Fig. 2b). At the slopes, the sum of the Lorentz and material forces are equal to F_1, F_2, respectively. In the subinterval where $a(t) = \text{const}$. the Lorentz force does not appear. However, it appears that the material force F_M depended on the instantaneous magnetic flux value (can be calculated by means of a static analysis $f = 0$). The horizontal part of the impulse is omitted (Fig. 2c, F_M is not regarded), but it is quite enough for presenting appropriate conclusions (Section 7). In order to evaluate force of a real impulse (Fig. 2b) the values of forces F_1, F_2 and F_M should be considered. Namely, considering the time period Δt where only material force F_M acts, the force equals $(F_1 t_1 + F_M \Delta t + F_2(t_2 - \Delta t))/(t_1 + t_2)$. For exponential impulse (Fig. 2c) is set $s = \pm 1/T$, because the derivatives on both slopes are determined by $\pm 1/T$, respectively. For such a shaped impulse the analytical solutions are obtained.

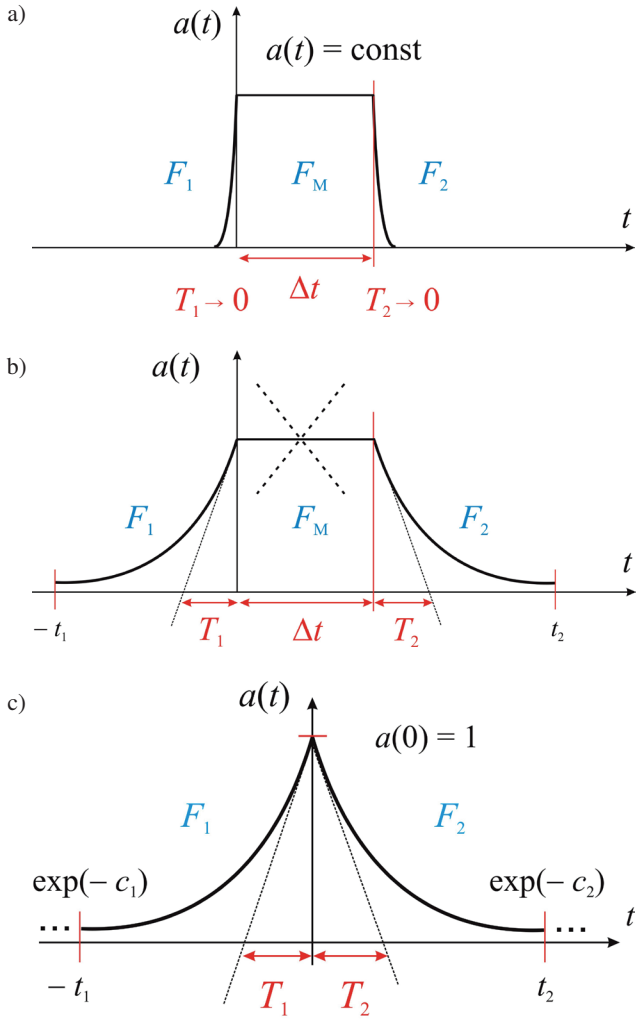

Fig. 2. a) ideal single impulse; b) technical realization of single impulse; c) single period of considered impulse function $a(t) = \exp(-t/T_1)$, $s_1 = 1/T_1$ for $t \in [-t_1, 0]$; and $a(t) = \exp(+t/T_2)$, $s_2 = -1/T_2$ for $t \in [0, +t_2]$

For exerted exponential–impulse periodic field and time functions $a(t) = \exp(\pm t/T_{1(2)})$ is satisfied $s_{1(2)} = \pm 1/T_{1(2)}$. The time period is equal to $\tau = t_1 + t_2 = c_1 T_1 + c_2 T_2$. For $c_1 = c_2 = c$, $T_1 = T_2 = T$, function $a(t)$ is continuous, and with the RMS value equal to

$$a_{\text{RMS}} = \sqrt{(1 - \mathrm{e}^{-2c})/2c}. \tag{10}$$

The variables separation method [1, 2, 20] allows for a general solution in the form as follows

$$A_\varphi(r, \theta) = \mathrm{R}(r)\mathrm{S}(\theta), \tag{11}$$

which leads to an equation

$$\frac{1}{r^2 \mathrm{R}} \frac{\partial}{\partial r}\left(r^2 \frac{\partial \mathrm{R}}{\partial r}\right) + \frac{\nu_{rr}}{\nu_{\theta\theta} r^2 \mathrm{S}} \frac{\partial}{\partial \theta}\left(\frac{1}{\sin\theta} \frac{\partial(\mathrm{S}\sin\theta)}{\partial \theta}\right) = \Gamma^2. \tag{12}$$

The separation with the constant $q$defined as

$$\frac{1}{\mathrm{S}} \frac{\partial}{\partial \theta}\left(\frac{1}{\sin\theta} \frac{\partial(\mathrm{S}\sin\theta)}{\partial \theta}\right) = -q, \tag{13}$$

and substitution of functions

$$\mathrm{Q} = \mathrm{S}\sin\theta\,, \tag{14}$$

leads to a differential equation

$$\sin\theta \frac{\partial}{\partial \theta}\left(\frac{1}{\sin\theta} \frac{\partial \mathrm{Q}}{\partial \theta}\right) = -q\mathrm{Q}. \tag{15}$$

The independent variable change $\theta = \arccos(x)$ ($x = \cos\theta$, $\theta \in (0, \pi)$) converts (15) into a differential equation

$$(1 - x^2) \frac{\partial^2 \mathrm{Q}_n}{\partial x^2} + q\mathrm{Q}_n = 0. \tag{16}$$

Solutions of (16) are trigonometric polynomials $\mathrm{Q}_n(x)$ defined for $q = q_n = n(n+1)$. Subsequently, polynomials $\mathrm{S}_n(x)$ are determined, which are proportional to associated Legendre polynomials $\mathrm{P}_n^1(x)$ [21].

The second variable term separated from (12) leads to the Bessel equations in the form of

$$\frac{\mathrm{d}^2 \mathrm{R}_n}{\mathrm{d}r^2} + \frac{2}{r}\frac{\mathrm{d}\mathrm{R}_n}{\mathrm{d}r} - \left(\Gamma^2 + \frac{q_n \nu_{rr}}{r^2 \nu_{\theta\theta}}\right)\mathrm{R}_n = 0. \tag{17}$$

The solution of Bessel equation for $\Gamma \neq 0$ [21] can be written in the form of

$$\mathrm{R}_n(r) = \frac{1}{\sqrt{\Gamma r}}\left(c_n \mathrm{I}_{p_n}(\Gamma r) + d_n \mathrm{K}_{p_n}(\Gamma r)\right), \tag{18}$$

where

$$p_n = \sqrt{\frac{1}{4} + n(n+1)\frac{\nu_{rr}}{\nu_{\theta\theta}}}. \tag{19}$$

For nonconductive and nonmagnetic ($\nu_{\theta\theta} = \nu_{rr} = \nu_0$) outer region of the ball at a low field frequency ($\Gamma_{\text{out}} \to 0$), the magnetic potential vector describes a function

$$\mathrm{R}_{0n}(r) = a_n r^n + b_n r^{-n-1}, \tag{20}$$

where a_n, b_n, c_n, d_n are constants.

For $n = 1, 2, \ldots$ functions $\mathrm{S}_1(\theta) = \sin\theta$, $\mathrm{S}_2(\theta) = \sin 2\theta, \ldots$ is the solutions ($d_n = 0$ because the field inside the ball must be limited) both inside the ball

$$A_\varphi(r,\theta) = \sum_{n=1}^{N} c_n \frac{\mathrm{I}_{p_n}(\Gamma r)}{\sqrt{\Gamma r}} \mathrm{S}_n(\theta), \tag{21}$$

and outside

$$A_{\varphi \mathrm{out}}(r,\theta) = \sum_{n=1}^{N} \left(a_n r^n + b_n r^{-n-1}\right) \mathrm{S}_n(\theta), \tag{22}$$

are enough developed in order to ensure fulfillment of all necessary boundary conditions for magnetic field [1, 2, 9, 17, 18, 22, 23]. Firstly, two constants result form parameters of given field, i.e. $a_1 = B_0/2$, $a_n = -C_{n-1}/2^n$ for $n = 2, 3, \ldots, N$. Secondly, two boundary conditions have to be satisfied for normal (radial) flux density B_r and for tangential (latitudinal) electric field strength E_θ. Hence

$$c_n = \frac{(2n+1)a_n R^n}{(\mu_0 \nu_{\theta\theta}) R \mathrm{G}_n(R) + n \mathrm{F}_n(R)}, \tag{23}$$

$$b_n = R^{n+1}\left(c_n \mathrm{F}_n(R) - a_n R^n\right), \tag{24}$$

where $\mathrm{F}_n(r) = \mathrm{I}_{p_n}(\Gamma r)/\sqrt{\Gamma r}$, $\mathrm{G}_n(r) = \partial(r\mathrm{F}_n(r))/r\partial r$.

Subsequently, basing on magnetic potential vector distributions (21) and (22), the magnetic and electric fields as well as current density are determined.

The solution presented for magnetically anisotropic ball generalizes the well-known force analysis for isotropic objects [5, 7, 9, 19].

4. Electromagnetic forces analysis: forces and power balances

The levitation force can be calculated by means of four following methods.

a) Maxwell stress tensor generalized method [1, 2, 5, 9, 18], which magnetic part is as follows

$$\vec{\sigma}_z = -H_z\vec{B} + \vec{i}_z(\vec{H}\vec{B})/2, \tag{25}$$

and leads to the force in the form of sum

$$F_z = F_{\mathrm{M}z} + \Delta F_z, \tag{26}$$

where integral over the sphere including the ball equals to

$$F_{\mathrm{M}z} = -\pi \int_0^\pi \mathrm{Re}\left\{-\frac{B_z^* B_r}{\mu_0} + \left(\frac{|B_r|^2}{2\mu_0} + \mu_0 \frac{|B_\theta|^2}{2\mu_{\theta\theta}^2}\right)\cos\theta\right\} R^2 \sin\theta \,\mathrm{d}\theta. \tag{27}$$

The additional summand ΔF_z can be simply evaluated by the following formula

$$\Delta F_z = \pi \int_0^\pi \int_0^R (\sigma_{\theta r} - \sigma_{r\theta}) \sin^2(\theta) r \,\mathrm{d}r \,\mathrm{d}r \,\mathrm{d}\theta. \tag{28}$$

The Maxwell stress method requires generalization [11, 17, 18] for regions where reluctivity is anisotropic, e.g. $\nu_{rr} \neq \nu_{\theta\theta}$. The total force calculated by means of Maxwell stress method must be extended by volume integral ΔF_z of non-zero value for anisotropic region (e.g. a ball). For isotropic regions $\Delta F_z = 0$.

Analogously, Maxwell stress tensor for electric field is considered and incorporated.

b) Co-energy method [1, 2, 9] requires calculating derivatives of magnetic and electric fields vectors in order to evaluate force $F_{\mathrm{C}z}$.

c) The Lorentz force $F_{\mathrm{L}z}$

$$F_{\mathrm{L}z} = \int_V \mathrm{Re}\left\{\left(\vec{J} \times \vec{B}^*\right)_z\right\} \mathrm{d}V = -\pi \int_0^\pi \int_0^R \mathrm{Re}\left\{\gamma E_\varphi B_\rho^*\right\} r^2 \sin\theta \,\mathrm{d}r \,\mathrm{d}\theta, \tag{29}$$

Moreover, the material force $F_{\mathrm{N}z}$ [1, 11] of the volume density on the ball acts as follows

$$\vec{N} = \frac{1}{2} B_u B_w \mathrm{grad}(\nu_{uw}) - \frac{1}{2} E_u E_w \mathrm{grad}(\varepsilon_{uw}), \tag{30}$$

where summation is performed. For diagonal anisotropy of the ball in the vacuum one obtains the surface force

$$F_{\mathrm{N}z} = \frac{\pi}{2} \int_0^\pi \left\{(\nu_0 - \nu_{rr})|B_r|^2 + (\mu_{\theta\theta} - \mu_0)|H_\theta|^2\right\} \cos\theta R^2 \sin\theta \,\mathrm{d}\theta + \frac{\pi}{2} \int_0^\pi (\varepsilon - \varepsilon_0)|E_\varphi|^2 \cos\theta R^2 \sin\theta \,\mathrm{d}\theta. \tag{31}$$

Both the Lorentz (29) and material (31) forces cover the total levitation force (Fig. 3).

d) Levitation force can also be calculated by means of equivalent dipole model [9, 19]). Namely, for $N = 2$ in (22) the magnetic flux density takes the form of

$$\vec{B} = \vec{i}_r 2\left(a_1 + \frac{b_1}{r^3}\right)\cos\theta - \vec{i}_\theta\left(2a_1 - \frac{b_1}{r^3}\right)\sin\theta = B_0\vec{i}_z + \underbrace{\vec{i}_r \frac{2b_1}{r^3}\cos\theta + \vec{i}_\theta \frac{b_1}{r^3}\sin\theta}_{\text{field of dipole}}, \tag{32}$$

and has the same form as that for the far field of single magnetic dipole [9, 19] with dipole moment equal to

$$m_{\mathrm{eff}} = 4\pi b_1/\mu_0, \tag{33}$$

thus, the force acting on dipole in gradient field is given by the formula as follows [18]

$$F_{Dz} = -\frac{1}{2}\mathrm{Re}\left(m_{\mathrm{eff}} C_1^*\right). \tag{34}$$

Eqs. (29) and (34) give the same results for an isotropic ball (if the magnetic field is dominant).

The forces evaluated by methods: a) Maxwell F_z (generalized), b) co-energy F_{Cz}, c) Lorentz F_{Lz} including material force F_{Nz} and d) equivalent dipol method (isotropic ball) are equal to each other

$$F_z = F_{Cz} = F_{Lz} + F_{Nz} = F_{Dz}, \tag{35}$$

if the Poynting force density

$$\vec{f}_P = \partial\left(\vec{D}\times\vec{B}\right)/\partial t, \tag{36}$$

vanishes [1, 2, 9, 11]. Nevertheless, the Poynting force F_{Pz} is calculated for checking the forces balance

$$F_{Pz} = -2\varepsilon F_{Lz}/\gamma T. \tag{37}$$

It should be additionally pointed out that contrary to the two methods a) and b), the third method c) bases on applying the physical force components, i.e. the Lorentz force density acting inside the ball and material forces acting upon the ball surface (at the boundary of the ball). Fig. 3 presents exemplary electromagnetic force distribution.

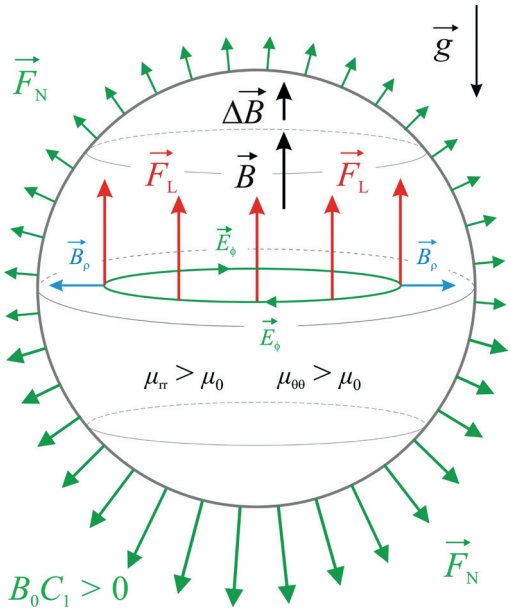

Fig. 3. Lorentz (antiparallel to g axis) and material (normal to ball surface) forces for para- and ferro-magnetics

The electromagnetic forces are calculated by means of Maxwell stress tensor (generalized) and the Lorentz force (including material forces) methods. Exemplary curves are shown in Figs. 4 and 5, where the complete sets of data are given in brackets.

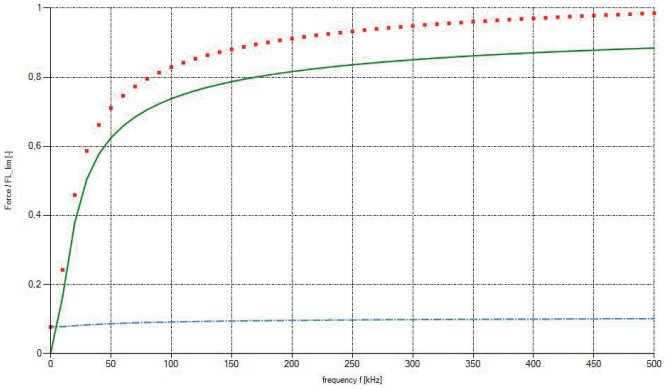

Fig. 4. Levitation force for conductive and magnetically isotropic ball evaluated by Maxwell stress tensor (points); Lorentz force (line) and material force (dash-dot line); $\Delta F = 0$ vs. frequency f ($R = 1.5$ mm; $\gamma = 35$ MS·m^{-1}; $s = \mathrm{i}\omega$; $\varepsilon = \varepsilon_0$; $\mu_{rr} = 0.9\mu_0$; $\mu_{\theta\theta} = 0.9\mu_0$; $B_0 = 0.5$ T; $C_1 = 10$ T·m^{-1}; $C_2 = 3\cdot10^3$ T·m^{-2}; $C_3 = 5\cdot10^5$ T·m^{-3}; $N = 4$)

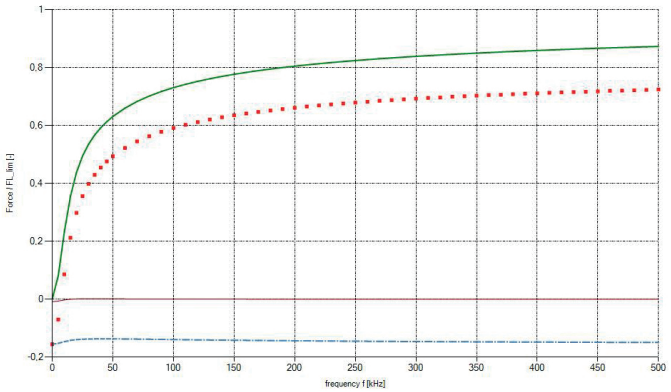

Fig. 5. Levitation force for conductive and magnetically anisotropic ball evaluated by Maxwell stress tensor (points); Lorentz force (line) and material force (dash-dot line); $\Delta F \neq 0$ (line nearest to the abscissa) vs. frequency f ($R = 1.5$ mm; $\gamma = 35$ MS·m^{-1}; $s = \mathrm{i}\omega$; $\varepsilon = \varepsilon_0$; $\mu_{rr} = 1.5\mu_0$; $\mu_{\theta\theta} = 1.2\mu_0$; $B_0 = 0.5$ T; $C_1 = 10$ T·m^{-1}; $C_2 = 3\cdot10^3$ T·m^{-2}; $C_3 = 5\cdot10^5$ T·m^{-3}; $N = 4$)

The fulfillment of power balance confirms the accuracy of the evaluated analytical solution field. The power balance can be written in the following form

$$S_P = \pi\int_0^{\pi}\left\{E_\varphi H_\theta^*\right\}R^2\sin\theta\,\mathrm{d}\theta = P_\gamma + 2(sE_\mu + s^*E_\varepsilon), \tag{38}$$

where power losses

$$P_\gamma = \pi\int_0^{\pi}\int_0^{R}\gamma|E_\varphi|^2 r^2\sin\theta\,\mathrm{d}r\,\mathrm{d}\theta, \tag{39}$$

magnetic field energy E_μ

$$E_\mu = \frac{\pi}{2}\int_0^{\pi}\int_0^{R}\left\{\nu_{rr}|B_r|^2 + \nu_{\theta\theta}|B_\theta|^2\right\}r^2\sin\theta\,\mathrm{d}r\,\mathrm{d}\theta, \tag{40}$$

and electric field energy E_ε

$$E_\varepsilon = \frac{\pi}{2}\int_0^\pi \int_0^R \varepsilon \left|E_\varphi\right|^2 r^2 \sin\theta \, \mathrm{d}r \, \mathrm{d}\theta \,. \tag{41}$$

Exemplary, the power balances are presented in Fig. 6 (diamagnetic ball) and Fig. 7 (paramagnetic ball).

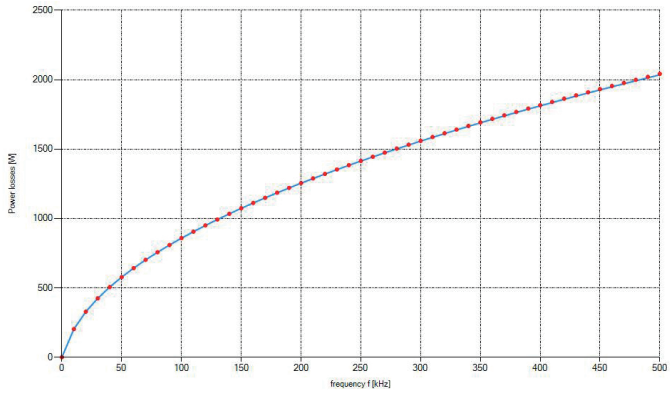

Fig. 6. Power losses evaluated by Joule volume integral (line) and Poynting vector surface integral (points) for levitating ball vs. frequency f ($R = 2$ mm; $\gamma = 56$ MS·m^{-1}; $\varepsilon = \varepsilon_0$, $\mu_{rr} = 0.95\mu_0$; $\mu_{\theta\theta} = 0.95\mu_0$; $B_0 = 0.7$ T; $C_1 = 10$ T·m^{-1}; $C_2 = 0$; $C_3 = 5 \cdot 10^5$ T·m^{-3}; $N = 4$)

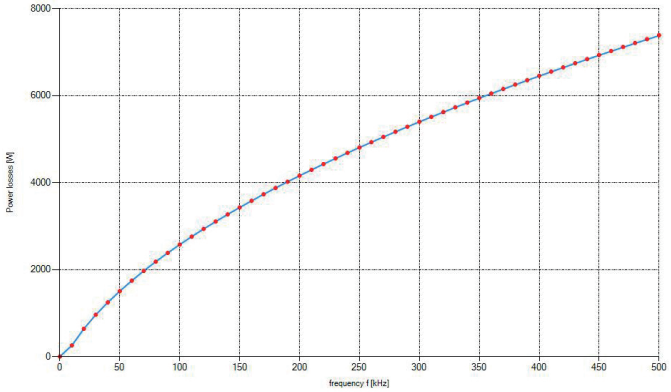

Fig. 7. Power losses evaluated by Joule volume integral (line) and Poynting vector surface integral (points) for levitating ball vs. frequency f ($R = 2$ mm; $\gamma = 10$ MS·m^{-1}; $s = \mathrm{i}\omega$; $\varepsilon = \varepsilon_0$; $\mu_{rr} = 2\mu_0$; $\mu_{\theta\theta} = 3\mu_0$; $B_0 = 0.7$ T; $C_1 = 10$ T·m^{-1}; $C_2 = 0$; $C_3 = 5 \cdot 10^5$ T·m^{-3}; $N = 4$)

5. High frequency asymptotic formulas for Lorentz force and power losses

For high frequency, so that $\mathrm{Re}\{\Gamma R\} \gg 1$, e.g. $\mathrm{Re}\{\Gamma R\} > 20$ for the Lorentz force and power losses can be presented by asymptotic formulas. The asymptotic formulas can be derived while using the approximation valid for any order ν

$$I_\nu(z) = \exp(z)/\sqrt{2\pi z}. \tag{42}$$

The Lorentz force asymptotic approximation for high frequency results directly from (29). The integrals over θ of summands including items of $E_\varphi B_r^*$, i.e. $\mathrm{S}_i(\theta)$, $\mathrm{dS}_k(\theta)$ and $\cos(\theta)\cdot\sin(\theta)$ for $i,k = 1,\ldots,N = 4$ lead to values grouped in the following matrix as follows

$$\mathbf{k}_{B_r} = \begin{bmatrix} 0 & 16/15 & 0 & 0 \\ -16/15 & 0 & 64/35 & 0 \\ 0 & -64/35 & 0 & 256/63 \\ 0 & 0 & -256/63 & 0 \end{bmatrix}. \tag{43}$$

The asymmetry of coefficients (43) results in zero value of the sum of all these integrals summand. However, the integrals over θ of summands including items of $E_\varphi B_\theta^*$, i.e. $\mathrm{S}_i(\theta)$, $\mathrm{S}_k(\theta)$ and $\cos(\theta)\cdot\sin(\theta)$ for $i,k = 1,\ldots,N = 4$ lead to the values grouped in the following matrix as follows

$$\mathbf{k}_{B_\theta} = \mathbf{k} = [k_{i,k}] = \begin{bmatrix} 0 & 8/15 & 0 & 0 \\ 8/15 & 0 & 64/105 & 0 \\ 0 & 64/105 & 0 & 64/63 \\ 0 & 0 & 64/63 & 0 \end{bmatrix}. \tag{44}$$

The symmetry of coefficients (44) leads to asymptotic formula as follows

$$F_{\mathrm{L}\max} = -\mathrm{Re}\left\{\sum_{n=1}^{N} \frac{\pi\gamma s(2n+1)(2n+3)}{\mu_{\theta\theta\mathrm{rel}}^{-2}\alpha\Gamma} k_{n,n+1} a_n a_{n+1} R^{2n+1}\right\}. \tag{45}$$

It should be pointed out that nonzero coefficients $k_{n,n+1}$ confirm that Lorentz force is derived only by two fields components (1) of the closest indices (n and $n+1$).

Figs. 8 and 9 show that forces increase vs. frequency and converge monotonically for $\mathrm{Re}\{\Gamma R\} \gg 1$. The Lorentz force asymptotic value is given by (45). Moreover, forces calculated by both Maxwell stress tensor and Lorentz methods (including material force) lead to the same results (Figs. 8 and 9) as is stated by (35). It should be pointed out that the levitation

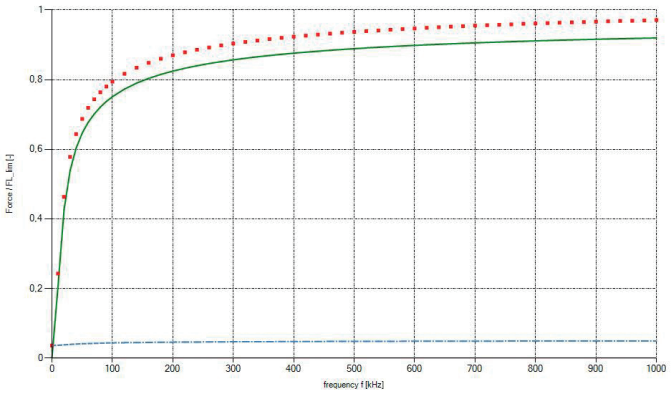

Fig. 8. Levitation force for conductive and magnetically isotropic ball evaluated by Maxwell stress tensor (points) and Lorentz force (line) including material force (dash-dot line near the abscissa); $\Delta F = 0$ vs. frequency f ($R = 3$ mm; $\gamma = 30$ MS·m^{-1}; $s = \mathrm{i}\omega$; $\varepsilon = 1.05\varepsilon_0$; $\mu_{rr} = \mu_{\theta\theta} = 0.9\mu_0$; $B_0 = 0.75$ T; $C_1 = 10$ T·m^{-1}; $C_2 = 0$; $C_3 = 4 \cdot 10^5$ T·m^{-3}; $N = 4$)

force reaches a certain maximal value. Hence, balls of limited mass can levitate in given excitation field only. The calculations of the forces have been brought out to the conclusions that Lorentz force is oriented vertically upwards when $B_0C_1 > 0$ (Fig. 1, $N = 2$). This inequality results from (45), too.

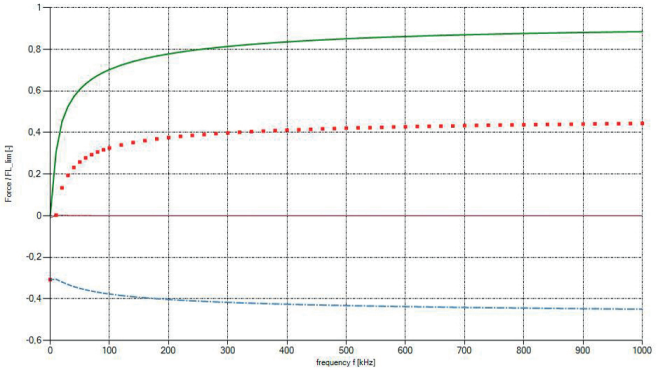

Fig. 9. Levitation force for conductive and magnetically anisotropic ball evaluated by Maxwell stress tensor (points) and Lorentz force (line) including material force (dash-dot line below the abscissa); $\Delta F \neq 0$ (line nearest to the abscissa) vs. frequency f ($R = 3$ mm; $\gamma = 10$ MS·m^{-1}; $s = \mathrm{i}\omega$; $\varepsilon = 1.05\varepsilon_0$; $\mu_{rr} = 3\mu_0$; $\mu_{\theta\theta} = 2\mu_0$; $B_0 = 0.75$ T; $C_1 = 10$ T·m^{-1}; $C_2 = 0$; $C_3 = 4 \cdot 10^5$ T·m^{-3}; $N = 4$)

The power losses asymptotic formula can be derived directly from volume integral (39). The integrals over θ of summands including items of $|E_\varphi|^2$, i.e. $\mathrm{S}_i(\theta)$, $\mathrm{S}_k(\theta)$ and $\sin(\theta)$ for $i,k = 1,\ldots,N = 4$ lead to values as shown in the following matrix

$$\mathbf{p} = [p_{ik}] = \begin{bmatrix} 4/3 & 0 & 0 & 0 \\ 0 & 16/15 & 0 & 0 \\ 0 & 0 & 32/31 & 0 \\ 0 & 0 & 0 & 128/45 \end{bmatrix}, \qquad (46)$$

where only diagonal coefficients $p_{n,n} = p_n$ are of nonzero values. Hence, the power losses by means of volume integral (39) after putting (21) and (42) are equal to

$$P_{\gamma\mathrm{limit}} = \pi |s|^2 \gamma \mu_{\theta\theta\mathrm{rel}}^2 \frac{1 - e^{-2\alpha R}}{2\alpha |\Gamma|^2} \sum_{n=1}^{N} (2n+1)^2 p_n a_n^2. \qquad (47)$$

Power losses can be evaluated based on surface integral of the Poynting vector over ball surface (38) as follows

$$P_{\gamma\mathrm{limit\,S}} = \pi \mu_{\theta\theta\mathrm{rel}}^2 \mathrm{Re}\{s/(\mu_{\theta\theta}\Gamma)\} \sum_{n=1}^{N} (2n+1)^2 p_n a_n^2. \qquad (48)$$

Both relations (47) and (48) are equivalent because for $\mathrm{Re}\{\Gamma R\} > 20$ is satisfied $\exp(-2\alpha R) \to 0$. In Figs. 10 and 11 the ratios of power losses to asymptotic approximation formulas (47) and (48) vs. field frequency are presented.

Fig. 11 pointed out graphically that power losses are proportional to the square root of field frequency

$$P_{\gamma\mathrm{limit}} / \sqrt{f} \approx \mathrm{const}, \qquad (49)$$

at a high frequency. This asymptotic property (49) results mathematically from both Eqs. (47) and (48).

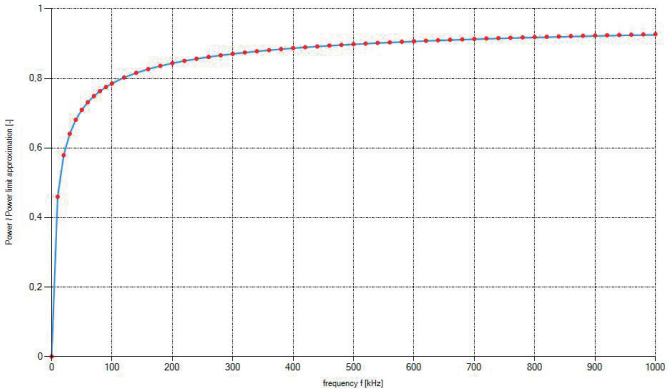

Fig. 10. Ratios of power losses P_γ both Joule losses (line) and Poynting vector surface integral (points) to asymptotic relation (48) for levitating ball vs. frequency f ($R = 3$ mm; $\gamma = 10$ MS·m^{-1}; $s = \mathrm{i}\omega$; $\varepsilon = 1.05\varepsilon_0$; $\mu_{rr} = 3\mu_0$; $\mu_{\theta\theta} = 2\mu_0$; $B_0 = 0.75$ T; $C_1 = 10$ T·m^{-1}; $C_2 = 0$; $C_3 = 4 \cdot 10^5$ T·m^{-3}; $N = 4$)

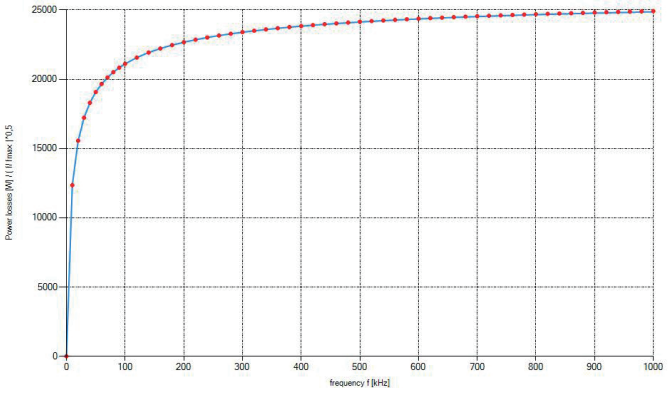

Fig. 11. Ratio of power losses P_γ both Joule losses (line) and Poynting vector surface integral (points) to frequency square root sqrt(f) vs. frequency f ($R = 3$ mm; $\gamma = 10$ MS·m^{-1}; $s = \mathrm{i}\omega$; $\varepsilon = 1.05\varepsilon_0$; $\mu_{rr} = 3\mu_0$; $\mu_{\theta\theta} = 2\mu_0$; $B_0 = 0.75$ T; $C_1 = 10$ T·m^{-1}; $C_2 = 0$; $C_3 = 4 \cdot 10^5$ T·m^{-3}; $N = 4$)

6. Forces acting on conductive, dielectric, and magnetic ball

Let us assume the field is stronger upside the ball. For paramagnetic and ferromagnetic balls (i.e. $\mu_{rr} > \mu_0$, $\mu_{\theta\theta} > \mu_0$) the whole material force acts downwards. The whole Lorentz force acts upwards (Fig. 12). The relation between these two forces depends strongly on the ball conductivity and frequency as shown in Figs. 13 and 14.

Both the whole Lorentz and material forces always act along z axis. Figs. 13 and 14 present the counteraction of the Lorentz and material forces for para- and ferromagnetics. The total force, i.e. the sum of Lorentz and material forces (equivalently given by Maxwell stress tensor generalized method) could be either positive (levitation is possible), negative, or equal to zero. On the contrary, for a diamagnetic ball both the Lorentz and material forces always coincide with each other and act towards the axis z.

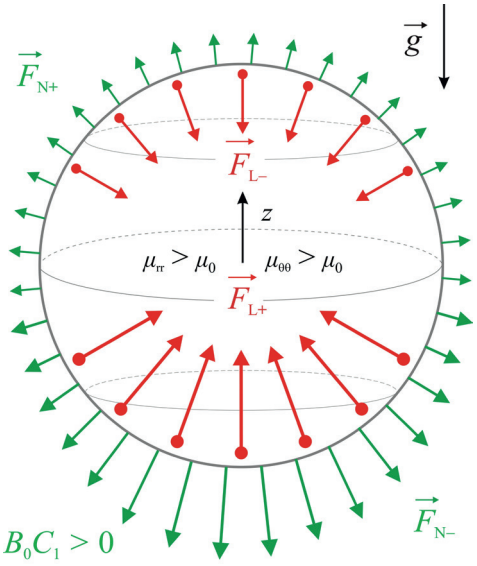

Fig. 12. Lorentz and material forces densities for para- and ferromagnetic ball

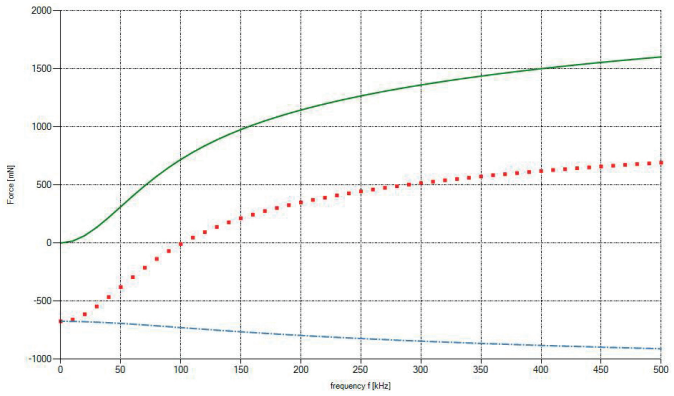

Fig. 13. Levitation force for conductive and magnetically anisotropic ball evaluated by Maxwell stress tensor (points); Lorentz force (line); material force (dash-dot line) vs. frequency f ($R = 3$ mm; $\gamma = 1$ MS·m^{-1}; $s = \mathrm{i}\omega$; $\varepsilon = \varepsilon_0$; $\mu_{rr} = \mu_{\theta\theta} = 2\mu_0$; $B_0 = 1$ T; $C_1 = 20$ T·m^{-1}; $C_2 = 0$; $C_3 = 5 \cdot 10^5$ T·m^{-3}; $N = 4$)

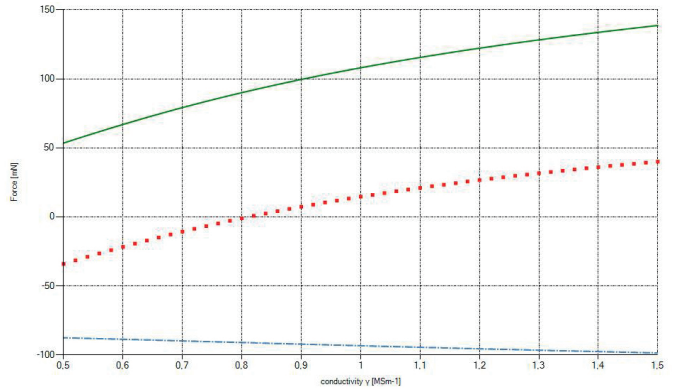

Fig. 14. Levitation force for conductive and magnetically isotropic ball evaluated by Maxwell stress tensor (points); Lorentz force (line); material force (dash-dot line) vs. conductivity γ ($R = 1.5$ mm; $f = 500$ kHz; $s = \mathrm{i}\omega$; $\varepsilon = \varepsilon_0$; $\mu_{rr} = \mu_{\theta\theta} = 2\mu_0$; $B_0 = 1$ T; $C_1 = 20$ T·m^{-1}; $C_2 = 0$; $C_3 = 5 \cdot 10^5$ T·m^{-3}; $N = 4$)

For impulse fields (Fig. 2) forces are either positive or negative or vanish, that means they may lead to levitation only for certain cases as shown in Figs. 15–17. These figures confirm that impulse levitation is not of practical interest.

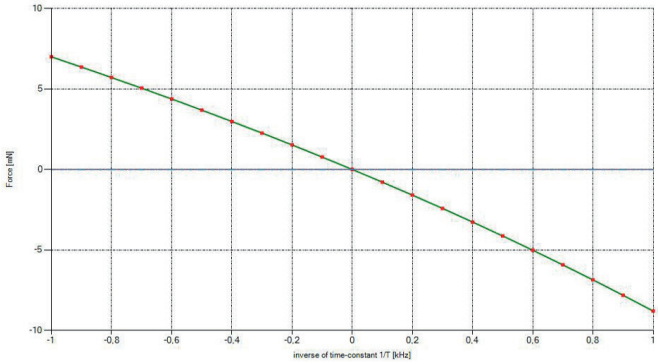

Fig. 15. Levitation force for conductive and nonmagnetic ball at impulse field evaluated by Maxwell stress tensor (points); Lorentz force (line); material force (dash-dot line) vs. time-constant inverse $1/T$ ($R = 5$ mm; $\gamma = 35$ MS·m^{-1}; $f = 0$; $s = \pm 1/T$; $\varepsilon = \varepsilon_0$; $\mu_{rr} = \mu_{\theta\theta} = \mu_0$; $B_0 = 0.5$ T; $C_1 = 5$ T·m^{-1}; $C_2 = 10 \cdot 10^3$ T·m^{-2}; $N = 3$)

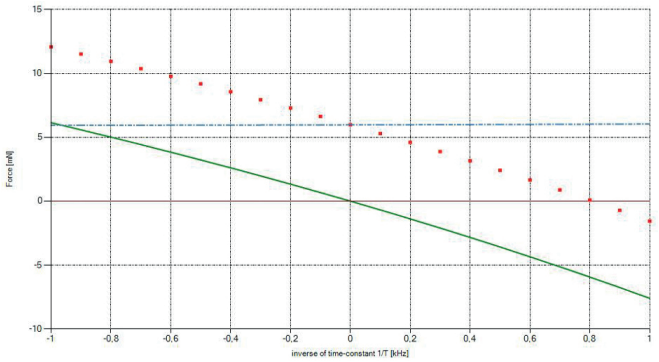

Fig. 16. Levitation force for conductive and magnetically isotropic ball at impulse field evaluated by Maxwell stress tensor (points); Lorentz force (line); material force (dash-dot line) vs. time-constant inverse $1/T$ ($R = 5$ mm; $\gamma = 35$ MS·m^{-1}; $f = 0$; $s = \pm 1/T$; $\varepsilon = \varepsilon_0$; $\mu_{rr} = \mu_{\theta\theta} = 0.9\mu_0$; $B_0 = 0.5$ T; $C_1 = 5$ T·m^{-1}; $C_2 = 10 \cdot 10^3$ T·m^{-2}; $N = 3$)

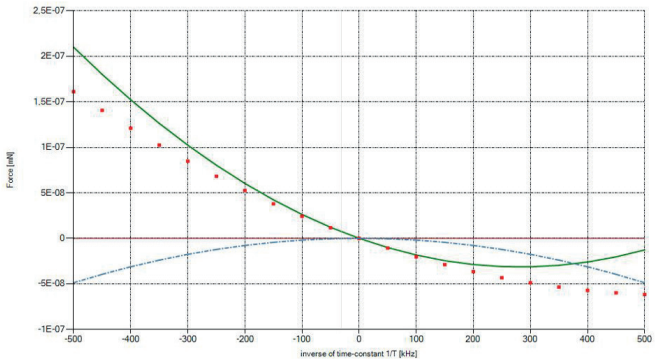

Fig. 17. Levitation force for conductive and magnetically isotropic ball at impulse field evaluated by Maxwell stress tensor (points); Lorentz force (line); material force (dash-dot line) vs. time-constant inverse $1/T$ ($R = 5$ mm; $\gamma = 5 \cdot 10^{-3}$ S·m^{-1}; $f = 0$; $s = \pm 1/T$; $\varepsilon = 100\varepsilon_0$; $\mu_{rr} = \mu_{\theta\theta} = \mu_0$, $B_0 = 0.5$ T; $C_1 = 5$ T·m^{-1}; $C_2 = 10 \cdot 10^3$ T·m^{-2}; $N = 3$)

7. Conclusions

The analytical solutions for electromagnetic field and forces of levitation problems for conductive, dielectric, and magnetic (anisotropic) ball have been presented. The ball is placed in either AC or impulse magnetic field (Fig. 2). The magnetic flux density is given in the form of polynomial (1) of N items.

The electromagnetic field distribution in a spherical coordinate system is determined by the separation of variables method. Provided analytical solutions satisfy Maxwell equations and boundary conditions for any ball parameters. The electromagnetic power balance for the obtained analytical solutions have been checked.

The electromagnetic forces (designed in order to ensure levitation) are evaluated by means of three methods, i.e. the Maxwell stress tensor (generalized [18]), co-energy and the Lorentz (including material forces [23]). All methods always give the same results (35).

Power losses are evaluated by means of the Joule power density and the Poynting vector.

The solutions derived are valid over a large frequency interval and ball parameters such as conductivity, magnetic permeability, radius, etc.

High frequency asymptotic formulas for the Lorentz force (45) and power losses (47) and (48) are derived.

The presented analytical solutions can be treated as benchmark tests for numerical algorithms for similar problems. Moreover, the proposed analytical solutions can be easily involved in electromagnetic field hybrid algorithms.

The analyses presented have been carried out based on the following:

- For para- and ferromagnetic ball both the Lorentz and material forces are acting against one another (AC field).
- For diamagnetic ball both the Lorentz and material forces always coincide (AC field).
- Total force can be positive for some conductivities, i.e. levitation is possible (Fig. 14, AC field),
- The Lorentz force asymptotic function (45) does not depend on frequency (Figs. 8 and 9, AC field),
- Power losses asymptotic function (49) depends on frequency square root (Figs. 10 and 11, AC field),
- Levitation for impulse field (Fig. 2) is nowadays out of practical interest due to either small or negative force value (Figs. 15–17).

References

[1] K.J. Binns, P.J. Lawrenson, and C.W. Trowbridge, *The analytical and numerical solution of electric and magnetic fields*, John Wiley & Sons, 1992.

[2] B.S. Guru and H.R. Hiziroglu, *Electromagnetic field theory fundamentals*, University Press, Cambridge, 2004.

[3] V. Dolga and L. Dolga, "Modeling and simulation of a magnetic levitation system", *Annals of the Oradea University of Timisoara, Romania*, VI (XVI) (2007).

[4] H. Górecki and M. Zaczyk, "Determination of optimal controllers. Comparison of two methods for electric network chain", *Bull. Pol. Ac.: Tech.*66 (3), 267–273 (2018).

[5] E. Fromm and H. Jehn, "Electromagnetic forces and power absorption in levitation melting", *British Journal of Applied Physics*, 16, 653–663 (1965).

[6] M. Zdanowski and R. Barlik, "Analytical and experimental determination of the parasitic parameters in high-frequency inductor", *Bull. Pol. Ac.: Tech.*65 (1), 107–112 (2017).

[7] E.C. Okress, D.M. Wroughton, G. Comenetz, P.H. Brace, J.C.R. Kelly, "Electromagnetic levitation of solid and molten metals", *J. Appl. Phys.* 23 (5), 545–552 (1952).

[8] D. Spałek, "Theorem about electromagnetic force surface representation in anisotropic region", *J. Tech. Phys.*XLVIII (3-4), 135–145 (2007).

[9] W.R. Smythe, *Static and dynamic electricity*, McGraw–Hill Book Company, New York, 1950.

[10] D. Spałek, "Electromagnetic torque components in synchronous salient-pole machine", COMPEL. *Int. J. Comput. . Math. Electr. Electron. Eng.* 16 (3), 129–143 (1997).

[11] D. Spałek, "Two theorems about surface-integral representation of electromagnetic force and torque", *IEEE Trans. Magn.* 53 (7), 1–10 (2017).

[12] W. He, J. Zhang, S. Yuan, A. Yang, and Ch. Qu, "Three-dimensional magneto-electric vibration energy harvester based on magnetic levitation", *IEEE Magn. Lett.* 8, 6104703 (2017).

[13] L. Ułanowicz and G. Jastrzębski, "The analysis of working liquid flow in a hydrostatic line with the use of frequency characteristics", *Bull. Pol. Ac.: Tech.* 68 (4), 949–956, (2020).

[14] T. Kaczorek, "Stability analysis of positive linear systems by decomposition of the state matrices into symmetrical and antisymmetrical parts", *Bull. Pol. Ac.: Tech.* 67 (4), 761–768 (2019).

[15] B.P. Mann and N.D. Sims, "*Energy Harvesting from the Nonlinear Oscillations of Magnetic Levitation*", Universities of Leeds, Sheffield and York (promoting access to White Rose research papers http://eprints.whiterose.ac.uk/), 2017.

[16] D. Spałek, "Analytical electromagnetic field and forces calculation for linear, cylindrical and spherical electromechanical converters", *Bull. Pol. Ac.: Tech.* 52 (3), 239–250 (2004).

[17] D. Spałek, "Levitation of Conductive and Magnetically Anisotropic Ball", *IEEE Trans. Magn.* 55 (3), 1000406 (2019).

[18] D. Spałek, "Generalization of Maxwell Stress Tensor Method for Magnetically Anisotropic Regions", *IEEE Trans. Magn.* 55 (12), 1000406 (2019).

[19] J.R. Wait, "A conductive sphere in a time varying magnetic field", *Geophysics*, 16 (4), 666–672 (1951).

[20] K. Jayasekera and I. Ciric, "Benchmark Computations of the Fields, Losses, and Forces for Conducting Spheroids in the Proximity of Current-Carrying Turns", *IEEE Trans Magn.* 42 (7), 1802–1811 (2006).

[21] I.S. Gradshteyn and I.M. Ryzhik, *Tables of Integrals, Series, and Products*, Academic Press, 2015.

[22] D. Spałek, "Fourth boundary condition for electromagnetic field problems", *J. Tech. Phys.* XLI (2), 129–144 (2000).

[23] D. Spałek, "Anisotropy component of electromagnetic force and torque", *Bull. Pol. Ac.: Tech.* 58 (1), 107–117 (2010).